Bulletin of the Seismological Society of America, Vol. 85, No. 5, pp. 1445–1455, October 1995

Waveform Inversion for Determining the Boundary Shape of a Basin Structure

by Shin Aoi, Tomotaka Iwata, Kojiro Irikura, and Francisco J. Sánchez-Sesma

Abstract We developed a method for estimating the boundary shape of a basin structure using seismograms observed on the surface. With this waveform inversion scheme, an accurate estimation is possible with data from a few surface stations, because seismic waves are affected not only by the local structure beneath the observation station but also by the entire basin structure. Numerical experiments were successfully carried out to determine the boundary shapes from observed surface records for a two-dimensional *SH* problem. For simplicity, only the boundary shape, that is thickness variations in the sedimental layer, was used as model parameters. This nonlinear problem is solved iteratively. To avoid the instabilities resulting from inappropriate initial models or from a large number of parameters, a hierarchical method, in which the number of parameters are increased gradually, is developed. We also successfully performed the inversions when the given parameters contain some errors and when the data contain noise.

Introduction

When seismic waves impinge on a basin from below, the seismic waves observed on the surface of that basin are affected by the physical properties and boundary shape of the basin. Ground motions of large amplitude and long duration are considered to be caused by the reverberation of S waves in soft sediments or to be surface waves generated secondarily at the basin's edges. In the 1985 Michoacan earthquake of M_S 8.1, Mexico City was severely damaged, although it is located more than 400 km from the epicenter. The damage was concentrated in a soft sediment area, the so-called lake zone. Compared with records from a surface station on a hill zone (bedrock) only 5 km from a lake-zone station, the peak accelerations recorded in the latter zone were about five times larger, and the duration was much longer (e.g., Beck and Hall, 1986). Many observations confirm the extraordinary effect of subsurface topography in other areas as well (e.g., Yamanaka *et al.*, 1989).

Many methods have been proposed for the calculation of synthetic waveforms in a laterally irregular structure: the Aki–Larner method (Aki and Larner, 1970), the finite-difference method (e.g., Boore, 1972), the finite-element method (e.g., Smith, 1975), and the boundary-element method (e.g., Sánchez-Sesma and Esquivel, 1979). Forward modeling performed with these methods has shown numerically that seismic waves of large amplitude and long duration occur (body waves amplified by soft sediments and surface waves generated secondarily at the edges of a basin) even for a simple body wave that impinges on the basin structure (e.g., Horike, 1987; Kawase and Aki, 1989). Furthermore, waveforms recorded on the surface have been shown to vary with the shape of the basin boundary (Bard and Bouchon, 1980).

The purpose of our study was to estimate the boundary shape of an underground structure by waveform inversion using seismograms observed on the surface. This is a type of domain/boundary inversion (Kubo, 1992), a method for estimating the boundary shapes of several regions regarded as homogeneous. The inversion using the shape of the boundary as the model parameters has already been studied in mechanical engineering. For example, there are some studies for detecting the shapes and locations of cracks from the static, or occasionally dynamic, responses of mass (e.g., Nishimura and Kobayashi, 1991; Tanaka and Yamagiwa, 1988). Another example is a study of the shape optimal problem (Barone and Caulk, 1982). In exploration geophysics, there have also been some attempts to estimate the boundary shape of the velocity discontinuity by applying the refraction (White, 1989) or the reflection method (Nowack and Braile, 1993) for the seismic wave. However, the resolution of the refraction method is low since it uses only a limited information at the arrival time. This does not fully utilize the information coming from the data. In the case of the reflection method, the data acquisition takes a long time since it spatially requires many observation data. Therefore, we will propose a method to estimate the underground structure by using the entire waveforms from earthquakes recorded at the small numbers of surface stations, including not only the direct waves but also the later phases.

In many cases of realistic geological structure, both sediment and basement layers are considered to be roughly homogeneous in the light of the high impedance ratio between them. Therefore, we assume that the basin structure discussed here is composed of two homogeneous layers divided by an irregular interface. We also assume that average velocities for the layers are known, and we seek to estimate the boundary shape. The boundary shape can be estimated directly from observed seismograms, using a small number of parameters to describe the boundary. We have assumed a two-dimensional problem and formulated a boundary shape waveform inversion for a plane *SH* wave impinging on a two-layered structure, and we have examined the validity of this inversion using numerical experiments. Inversions were performed for a given *S*-wave velocity and density for each layer and a given basin width. Since this is a nonlinear inverse problem, the solution is obtained by the linearized iterative method. To avoid computational instabilities (divergence or oscillation of the parameters) resulting from an inappropriate initial model or from a large number of parameters when the inversion is performed, the hierarchical method, in which the parameters are increased gradually, is proposed. We also performed the inversions when the assumed velocities are incorrect and when the data contain noise.

Effects of the Basin Structure on Seismic Waves Recorded on the Surface

To evaluate seismic waveforms on the surface when a plane *SH* wave impinges on a basin structure, we consider a basin structure model that consists of a homogeneous, isotropic, elastic layer underlain by a homogeneous, isotropic, elastic half-space. A two-dimensional (2D) *SH* problem is assumed, and the seismograms on the surface, when a plane *SH* wave impinges from the half-space, are calculated using the boundary-element method (Sánchez-Sesma *et al.*, 1993).

We investigated a basin structure (model 0 in Fig. 1 and Tables 1 and 2). Its width is 10.0 km, $\beta_1 = 1.0$ km/sec, $\beta_2 = 2.5$ km/sec, $\rho_1 = \rho_2$, and its maximum depth is 1.0 km. The boundary shape is a parabola (β represents the *S*-wave velocity and ρ the density, and the suffix depicts the layer number.). A plane *SH* Ricker wavelet (Ricker, 1977) with the characteristic frequency of f_c,

$$u(t) = (2\pi^2 f_c^2 t^2 - 1) \exp(-\pi^2 f_c^2 t^2), \qquad (1)$$

where $u(t)$ is displacement, was used as the incident wave. Seismograms on the surface when a Ricker wavelet with the characteristic period of 2 sec impinges on model 0 vertically from below are shown in Figure 2a. For simplicity, attenuation of the seismic wave in the propagation media is not considered in this investigation. Although the incident wave is a simple Ricker wavelet, its later phases are as equally prominent as direct waves. These later phases are surface

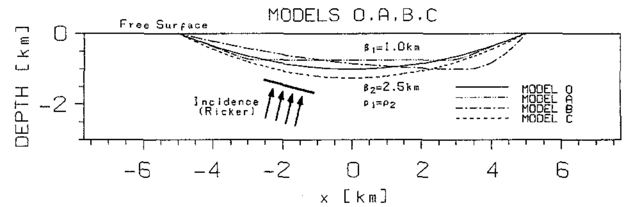

Figure 1. Basin structures of models 0, A, B, and C. The shear-wave velocities β_1 and β_2 are respectively 1.0 and 2.5 km/sec, and the density ρ_1 is given as equal to ρ_2 for these four models.

Table 1
Maximum Depths and Shapes of the Structure Models

	Shape	Max. Depth
Model 0	parabola	1.00 km
Model A	trapezoid	0.75 km
Model B	nonsymmetrical parabola	1.00 km
Model C	parabola	1.25 km
Width of basin	10 km	

Table 2
Physical Parameters of the Structure Models

	First Layer	Second Layer
S-wave velocity β	1.0 km/sec	2.5 km/sec
Q value	∞	∞
Density ρ	$\rho_1 = \rho_2$	

waves generated secondarily at the edges of the basin (e.g., Horike, 1987).

We performed a one-dimensional (1D) analysis to learn the influences of lateral heterogeneity on seismogram on the surface. We assumed a horizontally homogeneous, stratified structure based on the local structure beneath each surface station and calculated the surface waveform generated by a vertically incident *SH* wave from below by using the Haskell's method (Haskell, 1953). We call this a 1D analysis in the sense that it evaluates only the effect of the vertical heterogeneity. The synthetic waveform obtained by this 1D analysis (Fig. 2b) is composed of a direct body wave and small reverberations within the surface layer. The remarkable surface waves seen as later phases in the 2D analysis are not reproduced in the 1D analysis. Hence, when the structure varies laterally, the observed waveform on the surface is influenced not only by the local structure but by the entire structure. This suggests that if we use the full waveform, including the later phases, we may be able to estimate the entire structure for a two-dimensional problem using data from only a small number of stations. In contrast, if only the arrival time and direct wave are used, records from numerous stations are required to estimate the underground structure. The incident wave used in our numerical experiments, therefore, is a Ricker wavelet with a characteristic period of 2 to 3 sec, for which the surface wave generated secondarily becomes prominent for the basin structure model assumed.

Formulation of the Inversion

Basis Functions and Model Parameters for the Boundary Shape

We require a means of representing the boundary shape using a limited number of parameters. It is convenient if the boundary shape $\zeta(x)$ is represented by the basis function $c_k(x)$ and the real number parameter p_k as

$$\zeta(x) = \sum_k p_k \times c_k(x). \tag{2}$$

We therefore introduce the function system $\{c_k(x)|k = 1, 2, \ldots, K\}$,

$$c_k(x) = \begin{bmatrix} 1/2 + 1/2\cos\{\pi/\Delta(x - x_k)\} \\ 0 \end{bmatrix} \begin{matrix} \text{if } x_{k-1} \le x \le x_{k+1} \\ \text{otherwise.} \end{matrix} \tag{3}$$

The basin is located in the range of $-L < x < L$ and has a width of $2L$. The boundary is divided equally into $K + 1$ parts with $K + 2$ nodes [an interval $\Delta = 2L/(K + 1)$]. The first and last nodes being excluded, these K nodes are numbered from 1 to K. The x coordinate of the kth is denoted by x_k. Examples of the spatial distribution of the function system $c_k(x)$ for $K = 9$ are shown in Figure 3. The solid line represents $c_k(x)$ for $k = 4$. The boundary shape to be estimated, ζ, is denoted with this function system as

$$\zeta(x) = \zeta^0(x) + \sum_{k=1}^{K} p_k \times c_k(x), \tag{4}$$

where $\zeta^0(x)$ denotes the shape of the initial model. The parameter p_k physically represents the difference in depth between the target and initial models at x_k, $\zeta(x_k) - \zeta^0(x_k)$. The function system $c_k(x)$ interpolates the p_ks, giving the boundary depth at all discretized points.

Formulation of the Inversion

The observation equation is

$$u(x_m, t_n; \mathbf{p}) = \tilde{u}_{mn} \quad \text{(for all } m, n). \tag{5}$$

The left side, $u(x_m, t_n; \mathbf{p})$, is a synthetic waveform at the mth position, x_m, and the nth sampling time, t_n, for the vector of the model parameters $\mathbf{p}$ ($\mathbf{p} = (p_1, p_2, \ldots, p_K)$). The right side, $\tilde{u}_{mn}$, is the observed waveform (given) at x_m and t_n. The vector parameter $\mathbf{p}$ is determined to satisfy equation (5) in a least-squares sense.

As this is a nonlinear inverse problem, the solution is obtained by the linearized iterative method. A Taylor series expansion is performed on the left side of equation (5) about the parameter $\mathbf{p}^0$, where $\mathbf{p}^0$ is the vector of the model parameters for the initial $\zeta^0(x)$. By omitting the higher-order terms, this equation is linearized as

$$u(x_m, t_n; \mathbf{p}^0) + \sum_{k=1}^{K} \left.\frac{\partial u}{\partial p_k}\right|_{\mathbf{p}=\mathbf{p}^0} \delta p_k \simeq \tilde{u}_{mn}. \tag{6}$$

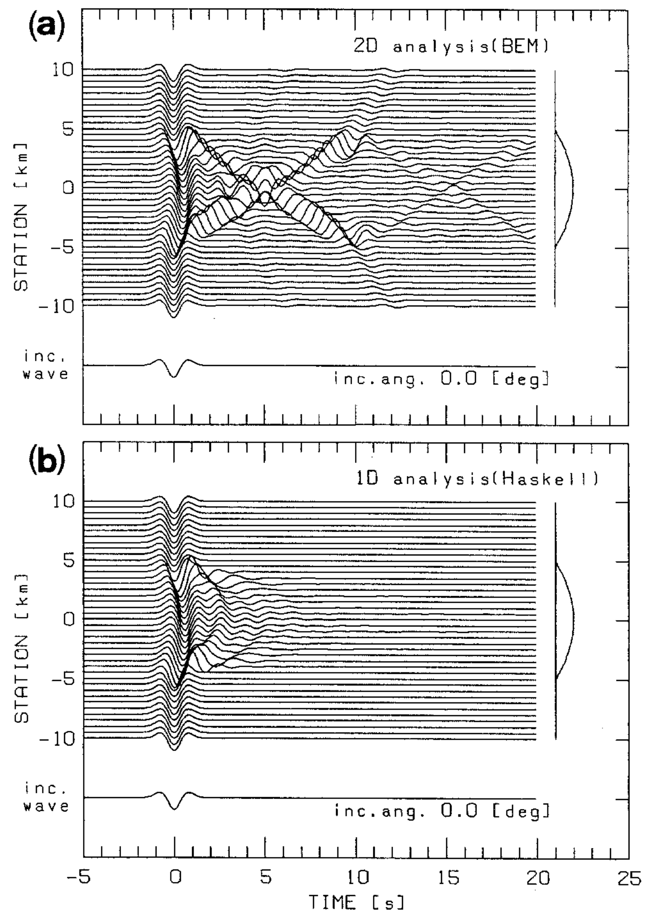

Figure 2. Synthetic seismograms at ground surface for model 0 for a Ricker wavelet with a characteristic period of 2 sec (vertical incidence). The underground structure is shown on the right side of the seismogram: (a) the 2D analysis (BEM) and (b) the 1D analysis (Haskell method). Although there is similarity in the direct wave part in both figures, the surface waves are predominant only in the 2D case.

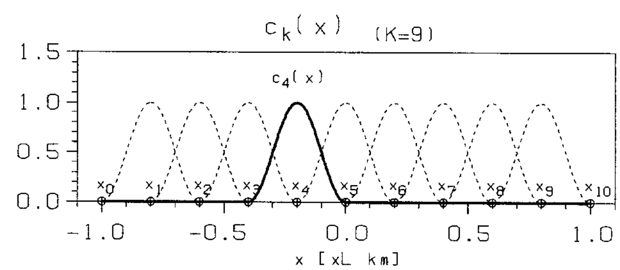

Figure 3. Examples of the space distribution of the weight function system $c_k(x)$ when $K = 9$. Solid line shows the example of $c_k(x)$ for $k = 4$.

Because the differential seismogram $\partial u/\partial p_k$ cannot be obtained analytically, we replace it with a finite-difference approximation. Approximating equation (6) with finite differences, we obtain

$$\sum_{k=1}^{K} \frac{u(x_m, t_n; \mathbf{p}^0 + \Delta\mathbf{p}_k) - u(x_m, t_n; \mathbf{p}^0)}{\Delta p_k} \delta p_k \simeq \tilde{u}_{mn} - u(x_m, t_n; \mathbf{p}^0), \quad (7)$$

where Δp_k is an appropriate positive number, and $\Delta\mathbf{p}_k = (0, \ldots, 0, \Delta p_k, 0, \ldots, 0)$. Equation (7) is a set of simultaneous linear equations whose coefficient matrix is nonsquare. We use the singular value decomposition method to solve this equation (e.g., Aki and Richards, 1980; Nakagawa and Oyanagi, 1982).

In the inversion process described, the correction value for each parameter is determined. Using this value, we construct the starting model for the next iteration. The square sum, $\sum_{m,n}[\tilde{u}_{mn} - u(\mathbf{p})]^2$, of the residuals between the data and synthetic seismograms is used to check the degree of fit of the models. The solution that converges by the use of this linearized iterative method is considered the best model when the residuals are sufficiently small.

To perform a nonlinear inversion with an iterative method, an appropriate initial model that consists of *a priori* information is necessary. This is a problem that we have to face inevitably, and without enough *a priori* information, the inversion cannot be performed. However, in many cases, we have some information of the underground structure given by the borehole logs, gravity exploration and seismic exploration, such as reflection method and refraction method. These pieces of information often enable us to construct an appropriate initial model, with which we can estimate a basin structure with seismic data.

Differential Seismograms

When inversion of a boundary shape is performed using seismograms on the surface, the coefficient matrix of the linearized observation equation $\Sigma\ \partial u/\partial p_k \cdot \delta p_k \simeq \tilde{u} - u(\mathbf{p}^0)$ is required. As stated earlier, $\partial u/\partial p_k$, the differential seismogram, is replaced by the finite difference $\Delta u/\Delta p_k$ in our method. This represents a sensitivity of a change in the waveform that corresponds to the change of the kth model parameter p_k.

The case discussed here has nine model parameters ($K = 9$). Figure 4 shows the time and space distributions of the differential seismograms that correspond to the waveforms in Figure 2a; the differential coefficient $\Delta u/\Delta p_k (k = 1 \sim 5)$ corresponds to the coefficient of $\delta p_1 \sim \delta p_5$. These differential seismograms are calculated with $\Delta p_k = 5 \times 10^{-3}$ km; i.e., $\Delta p_k/L = 10^{-3}$, since $L = 5$ km. This is considered to be a good approximation of $\partial u/\partial p_k$ because the value of Δp_k is sufficiently small compared with the width of the basin and the maximum depth (1 km). Moreover, the finite-difference value, $\Delta u/\Delta p_k$, is almost constant in the range of $\Delta p_k/L = 10^{-2} \sim 10^{-4}$. Figure 4 indicates that lateral change in the layer depth influences not only the direct waves above but also secondarily generated surface waves of the seismograms at all the surface stations. In addition, the change in depth near the edge of the basin has a greater effect on the surface seismograms than does the change in depth in the central part of the basin (e.g., compare Figs. 4a and 4e). The fact that the time and space distributions of $\Delta u/\Delta p_k$ totally differ depending on k suggests the possibility that we can invert the model parameters with sufficient resolution.

The differential coefficient $\Delta u/\Delta p_k$ is obtained by repeated computation of synthetic waveforms by forward modeling for many perturbed structures. When the boundary-element method is used, the most significant part of the computation consists of obtaining the Green's functions. Computation of the Green's functions is needed again only for those corresponding to the perturbed parts of the structures. The computation time needed for the inversion therefore can be greatly reduced because the same process is not repeated when local parameters are used.

Hierarchical Scheme of Inversion

When performing the inversion, computation becomes unstable (it means that parameters diverge or oscillate) if the given initial model is not appropriate or the number of parameters is too large. In such cases, a hierarchical scheme of inversion can improve the unstable computation. Though it is unnecessary to use the hierarchical method when an initial model is known to be appropriate, the use of this method is not harmful, which just requires more steps in the inversion. In all other cases, this method is useful in stabilizing the computation.

Appropriate Initial Model

A boundary shape can be estimated even from a few surface stations when the inversion is performed with an "appropriate" initial model, as described in detail in the next section. An appropriate initial model here means that $\Delta\zeta_{max}$ is small enough compared with ζ_{max},

$$\Delta\zeta_{max} = \max_x |\zeta(x) - \zeta^0(x)|,$$

where $\zeta^0(x)$ and $\zeta(x)$ respectively are the depths of the initial and target models and ζ_{max} is the maximum depth of the sediment. Obviously, to select an appropriate initial model, one must incorporate all available *a priori* information about the basin.

In solving this kind of nonlinear inverse problem, use of an inappropriate initial model leads to divergence or oscillation of the parameters in the early steps of iteration, and this unstable computation makes it difficult to extract the information contained in the data.

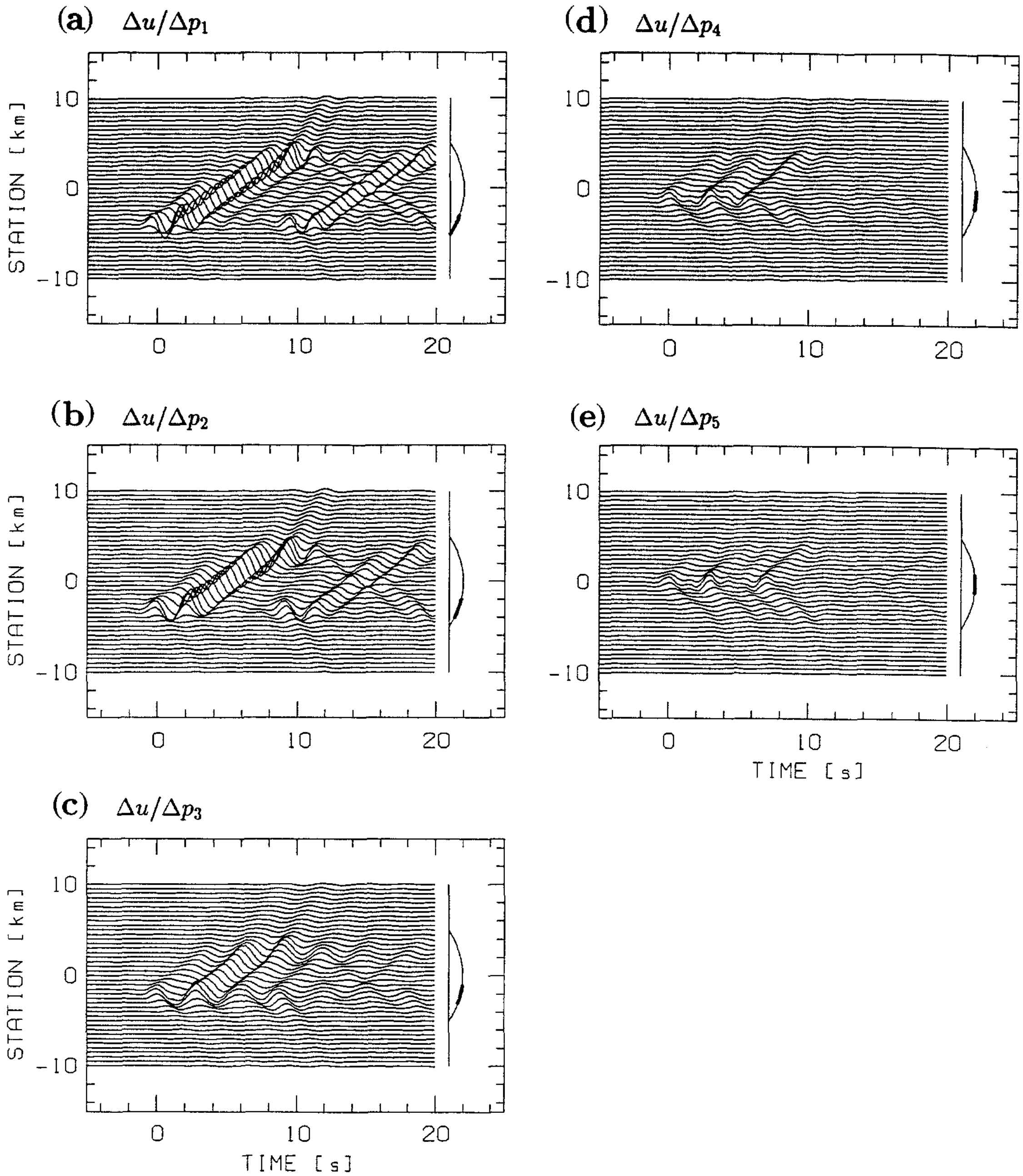

Figure 4. Differential seismograms $\Delta u/\Delta p_k$ of model 0 for $K = 9$. (a), (b), (c), (d), and (e) correspond to $k = 1, 2, 3, 4$, and 5, respectively.

Hierarchical Scheme

Since the inversion tends to be unstable when there are many parameters, we introduced a hierarchical scheme (e.g., Kubo *et al.*, 1988). This is a scheme to perform a stable inversion without losing the resolution of the data: First, inversion is performed iteratively with a small number of parameters until the residuals converge, then the number of parameters is increased. For each increase in the number of parameters, additional iterations are made until the residuals again converge. Eventually the residuals stop decreasing, in spite of the increase in the number of parameters, when the number of parameters required to reproduce the target model is reached. The minimum number of parameters required to match the observation can be estimated roughly in this way.

Numerical Tests of Inversion Method

In our numerical experiments, we use waveforms synthesized from a target model as pseudo-observed data in order to show the usefulness of boundary shape inversion.

Models A and B in Figure 1 and Table 1 are the target models. The physical constants of each layer in both models are listed in Table 2. Our data consist of the synthesized waveforms taken from several stations on the surface within the basin, computed assuming an incident plane *SH* wave with a Ricker wavelet time function.

The *S*-wave velocity and density for each layer, the width of the basin, and the angle and pulse shape of the incident wave, assumed to be given without error, are given as *a priori* information. The case in which there are errors in these parameters is discussed later. For simplicity, the attenuation in propagation is not considered in this study, and the *Q* values for both layers are given as infinite. Otherwise, the *Q* values could be parameters to be estimated, although perhaps not uniquely. We used model 0 as the initial model, as described in Figure 1 and Tables 1 and 2.

Case A: Model A as the Target Model

The solid lines in Figure 5 show the waveforms synthesized for three surface stations, using a Ricker wavelet with a characteristic period of three seconds impinging on Model A vertically from below. The data length is 8.7 sec, from − 1.9 to 6.8 sec (sampling rate is 12.8 Hz). The broken lines show the waveforms synthesized from the same incident wave that impinges on the initial model.

These waveforms were used as pseudodata in the inversion with nine model parameters ($K = 9$). The estimated models and the residuals of each iteration step are shown respectively in Figures 6 and 7. The residuals are normalized by that of the initial model. The residual decreases until the fourth iteration, becoming almost constant thereafter. The target model is estimated exceptionally well by the fourth iteration.

Thus, under ideal conditions, the shape of an entire structure can be estimated with data from only a few surface stations when the full waveforms, including the later phases, are used.

Case B: Model B as the Target Model

In this case, our target is model B, and the initial model (model 0) is not as close to the target model as it was in case A; therefore, the hierarchical scheme is used. The basin of the target model has a smooth, lateral gradient in thickness, which increases to a maximum depth of 1.25 km and truncates sharply near the right side of the model. The solid lines in Figure 8 show waveforms synthesized for four surface stations using a Ricker wavelet with a characteristic period of 3 sec impinging on model B at the incident angle of 15° to the left of the vertical line. The data length is 16.4 sec, from − 1.9 to 14.5 sec (sampling rate, 12.8 Hz). The broken lines show the waveforms synthesized from the same incident wave that impinges on the initial model, model 0. The waveforms shown by the solid and broken lines differ markedly. This indicates that the initial (model 0) and target (model B) models are not likely to be close.

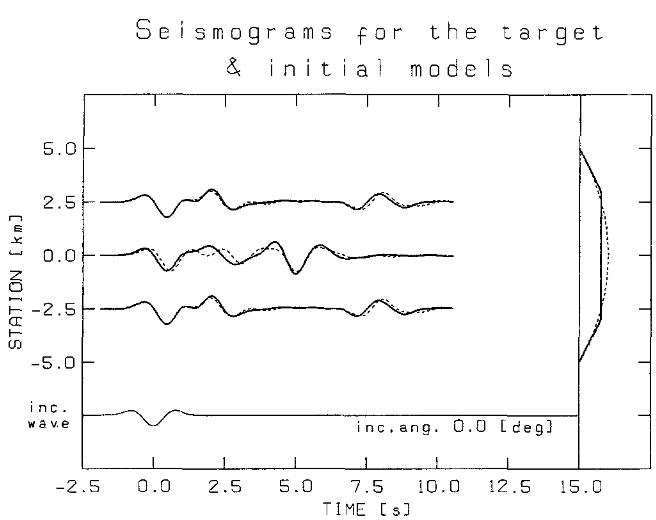

Figure 5. Seismograms recorded at three surface stations for the target (model A) and initial (model 0) models shown respectively by solid and broken lines. They were produced by a Ricker wavelet with a characteristic period of 2 sec impinging on the models vertically from below. The incident wave is shown in the bottom trace.

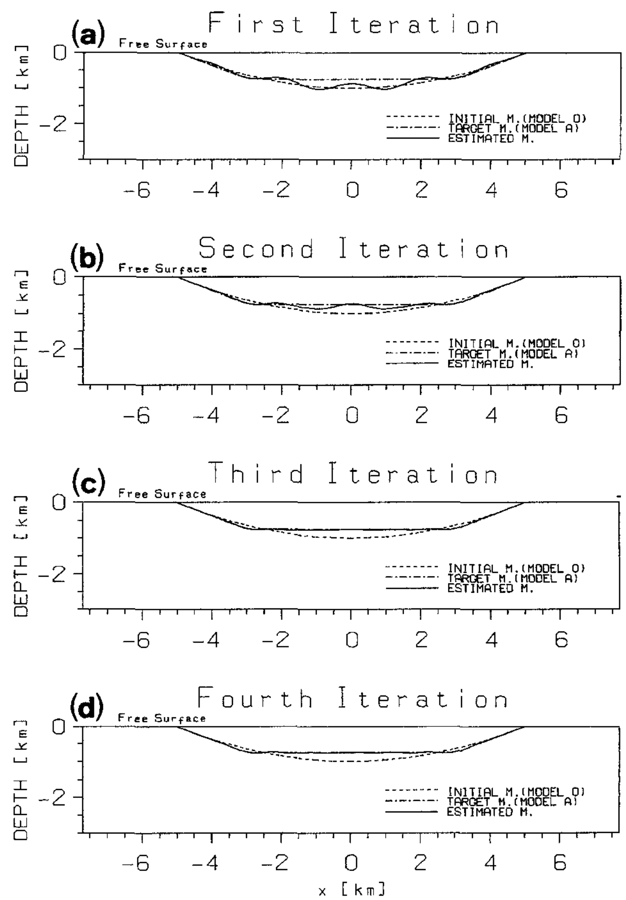

Figure 6. Results of the inversion. The initial (model 0), target (model A) models, and estimated models obtained by the first, second, third, and fourth iterations are shown respectively by (a), (b), (c), and (d).

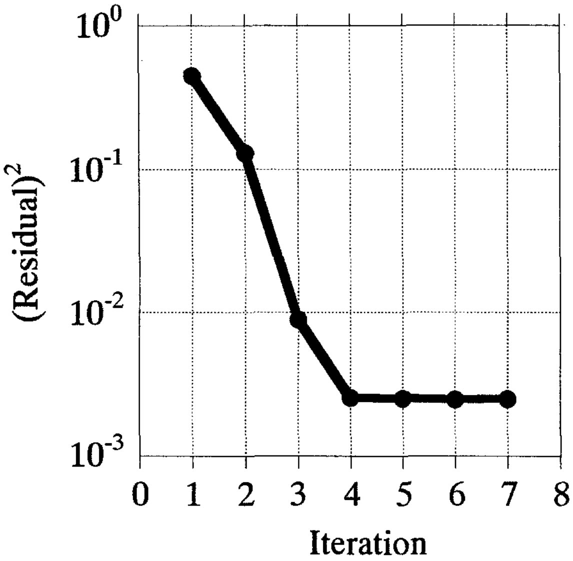

Figure 7. Change of the square sum of the residuals after each iteration for the inversion in case A. The residuals are normalized by that of the initial model. They decrease monotonically and converge at the third iteration.

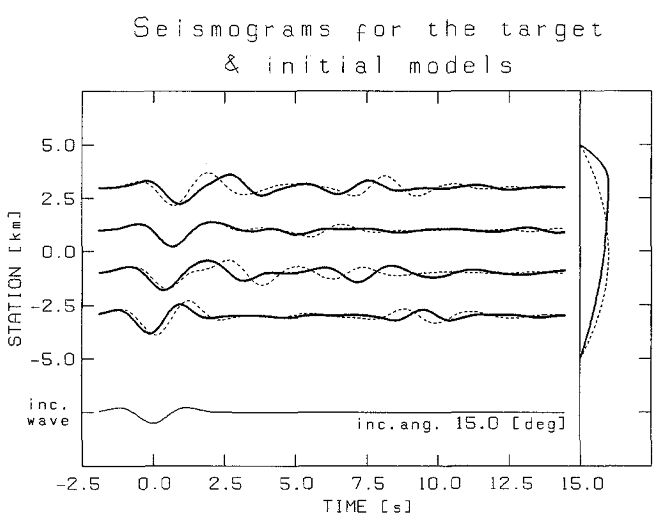

Figure 8. Seismograms for the target (model B) and initial (model 0) models shown respectively by solid and broken lines. They were produced by a Ricker wavelet with a characteristic period of 3 sec impinging on the models from below at an angle of 15° to the left.

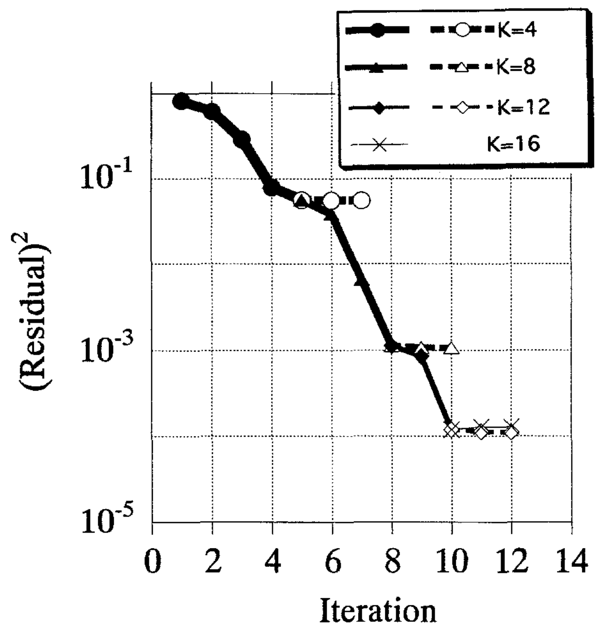

Figure 9. Change in the square sum of the residuals after each iteration in the inversion for case B. The residuals are normalized by that of the initial model. In the hierarchical scheme, the number of parameters is increased by four each time the residuals converge.

Using these waveforms, we first performed the inversion with four parameters ($K = 4$). The residual of each iteration step is shown in Figure 9. The residual decreases until the fourth iteration, becoming almost constant thereafter. After the fourth iteration, the number of model parameters is increased from 4 to 8, after the 8th iteration to 12, and after the 10th to 16. As the parameters are increased by fours from 4 to 12, the residuals decrease; yet, there is no further decrease when the parameters are increased to 16. This means that the data can be explained by a model with 12 parameters.

In each step of the hierarchical inversion, the estimated model is compared with the target model (Fig. 10). Even with four parameters, the left half of the structure is well estimated (Fig. 10a); the right half is not so well estimated because these four parameters cannot express the steep edge of model B. An increase of number of the parameters to 8 improves the estimation of the right side (Fig. 10b). With 12 parameters, the entire target model, including the right side, is estimated almost perfectly (Fig. 10c). In this case, 12 parameters sufficiently reproduce the model, which is consistent with earlier results for the convergence of residuals.

We conclude that when the hierarchical scheme is used, larger range of model parameters can be used for the initial model.

Further Tests with Noise and with Errors

Numerical experiments showed that the entire boundary shape can be estimated with noise-free data from only a small number of surface stations when the full waveforms including the later phases are used and when there are no errors in the initial velocity assumptions. Here, we discuss the effects of two types of errors (noise contained in the data and errors in the given parameters: the assumed velocity and incident angle) on inversion results.

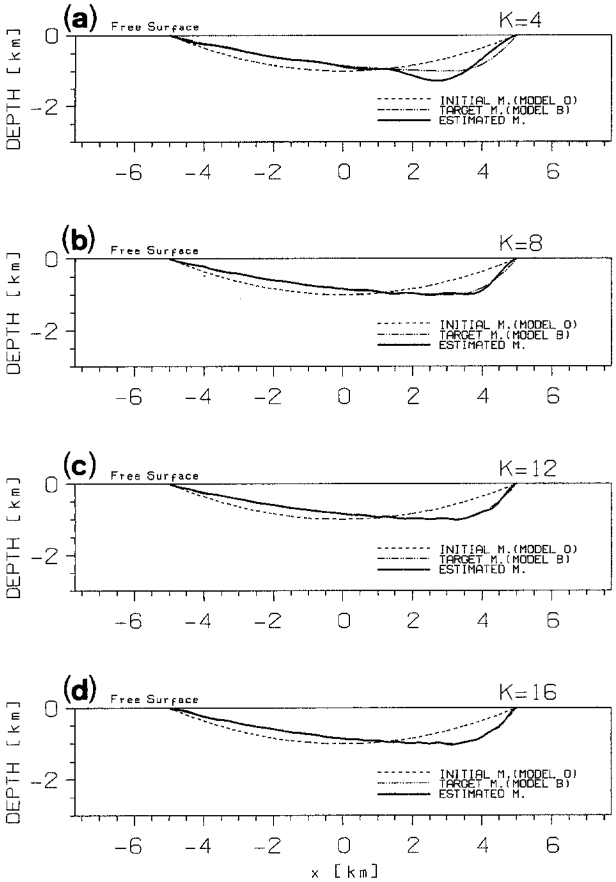

Figure 10. Results of the inversion. (a) through (d) show the initial (model 0), target (model B), and estimated models at each step of the hierarchy.

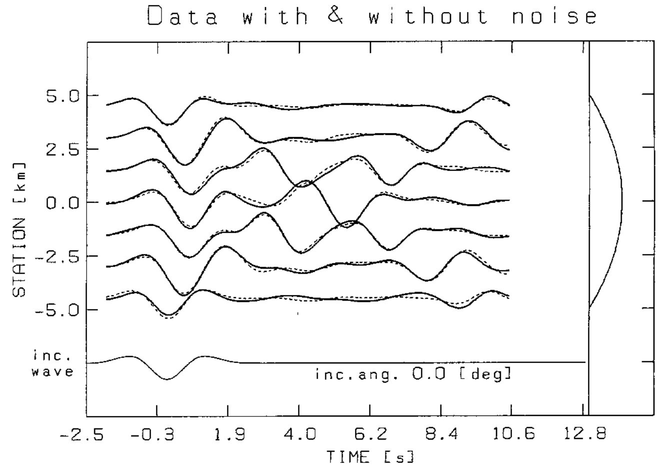

Figure 11. Data used to examine the effects of noise on inversion. Broken line: data without noise. Solid line: data with Gaussian noise with zero mean and normal distribution bandpass-filtered between 2 and 5 sec.

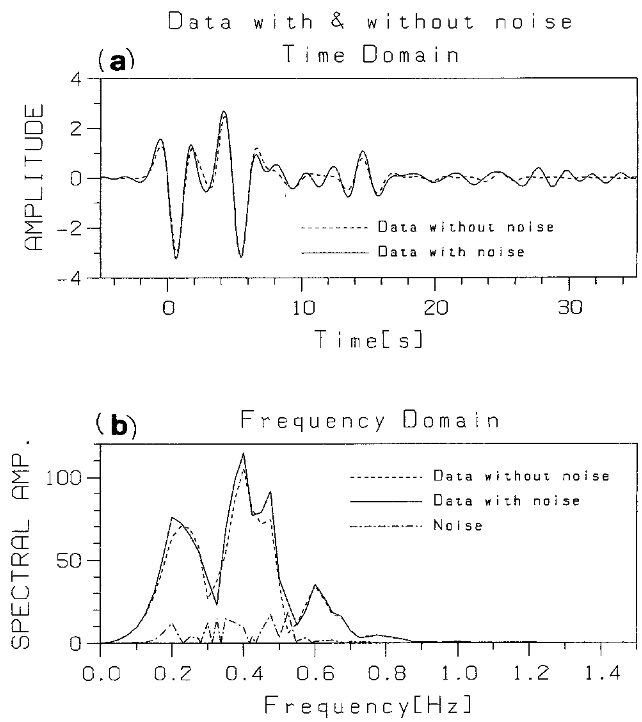

Figure 12. Data with (broken line) and without (solid line) noise at the center of the basin ($x = 0$) in the (a) time and (b) frequency domains.

Effects of Noise in the Data

Inversion is performed with data to which Gaussian noise has been added artificially in order to examine the effects of noise. The data were a wave field generated by a Ricker wavelet that has power in a very narrow band in the frequency domain. Therefore, Gaussian noise of zero mean and normal distribution is bandpass-filtered in the bandwidths 2 to 5 sec, and then added to the data to include noise.

The target model, model C, is shown in Figure 1 and Tables 1 and 2. The broken line in Figure 11 shows waveforms (without noise) synthesized from a Ricker wavelet with a characteristic period of 3 sec, impinging vertically on model C from below. The data constructed by adding noise to these waveforms are shown by the solid line in the same figure. Figures 12a and 12b respectively show the waveforms at the center of the basin in the time and frequency domains. When the noise ratio is defined as $\Sigma|\text{noise}|/\Sigma|\text{data}|$ in the frequency domain, the noise ratio for the data in Figure 11 is approximately 12%.

Results of the inversion are shown in Figure 13; model 0 was used as the initial model. The model is successfully estimated when $K = 4$ and $K = 8$. The fact that the model can also be estimated with data containing noise reveals the significant potential of this method for dealing with real data. But for a large number of parameters, such as $K = 12$, small fluctuations that do not exist in the target model appear in the estimated model. These fluctuations occur because the number of parameters was increased beyond the amount of information contained in the data. The appropriate number of parameters therefore must be determined from the S/N ratio. The hierarchical inversion approach is ideally suited to select an appropriately parameterized model. Statistical tests, such as the Akaike information criterion [(AIC) e.g., Nakagawa and Oyanagi, 1982] or the Akaike Bayesian information criterion (ABIC) could be used to select an appropriate number of model parameters.

Errors in Given Parameters

In the numerical tests discussed earlier, we assumed that parameters such as the S-wave velocity, density, and incident angle are known, except for the parameters of boundary shape. Actually, such given parameters contain certain errors. Therefore, we examined the effects on the inversion results by an error in S-wave velocity and by an error in incident angle.

In the first example, the S-wave velocity of the first layer is given as 5% faster than the true value. The data used for the inversion are the synthetic waveforms generated by a Ricker wavelet with a characteristic period of 3 sec impinging vertically on model C from below (Fig. 14). The same model 0 was used as the initial model, except for $\beta_1 = 1.05$ km/sec. As shown in Figure 15, the results closely reflect the true structure, but it is estimated to be about 10% deeper than the target structure. Since a trade-off exists between velocity and depth (Ammon *et al.*, 1990), it is difficult to determine the absolute value of seismic wave velocity and the depth of the structure simultaneously in most seismic exploration methods, although there are some attempts to separate them (Olsen, 1989). The estimation of a deeper structure when an erroneously fast seismic wave velocity is assumed is therefore expected.

The second example is for an error in the incident angle. The data obtained from model C are used, and the inversion was performed with model 0 as the initial model. The given incident angle is vertical, whereas the true incident angle is 5° to the left. The results of inversion shown in Figure 16 closely reflect the true structure, but the left half of the inverted boundary shape is estimated to be shallower and the right half deeper than the target. This is due to the phase shifts created by the error in the assumed incident angle: On the left side of the basin, the phases shift later than the true ones, whereas the phases shift earlier on the right side.

Although the noise contained in the data and the errors in the given parameters affect the estimations, our tests suggest that the models can be roughly estimated as long as the noise in the records used in the inversion is less than 15% and the errors of S-wave velocity and the incident angle are respectively within 5% and 5°.

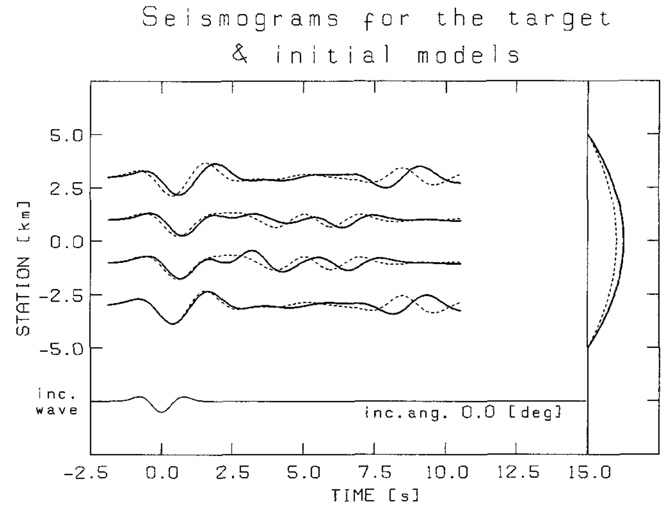

Figure 14. Seismograms recorded at four surface stations for the target (model C) and initial (model 0) models shown respectively by solid and broken lines. They were produced by a Ricker wavelet with a characteristic period of 3 sec impinging on the models vertically from below.

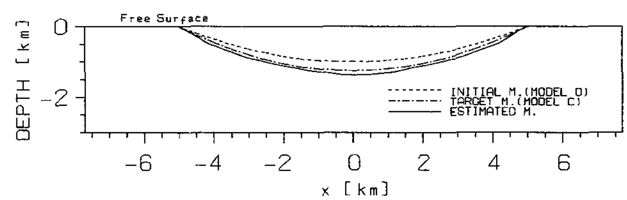

Figure 15. Results of inversion with model 0 as the initial model but with $\beta_1 = 1.05$ km/sec. The estimated model closely reflects the target structure but is estimated as being deeper than the target.

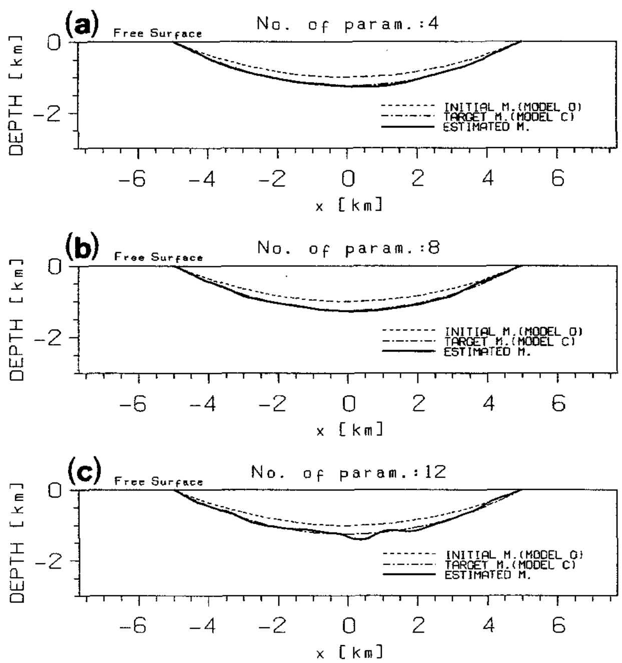

Figure 13. Results of inversion with data containing noise. The correct model can be estimated with data containing noise (a) and (b), but undesirable fluctuation occurs when too many parameters are introduced (c).

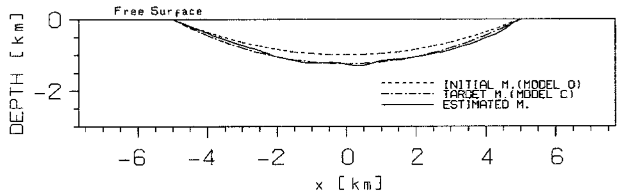

Figure 16. Results of inversion with model 0 as the initial model when the given incident angle is vertical, whereas the true incident angle is 5° to the left. The estimated structure closely reflects the target structure, but the left half is estimated as being shallower and the right half as being deeper than the target.

Discussion

A question of extending this method to 3D structures remains, since we cannot actually expect an ideal 2D structure, though a 2D *SH* problem was assumed for this study. Nevertheless, the wave fields in some basin structures were well explained by the 2D forward modeling (e.g., Yamanaka *et al.*, 1989, 1992). In these cases, the 2D problems are significant for realistic applications. Moreover, the formulation in the basic 2D problems is useful as the first step, which can then be extended to invert fully 3D structures.

When the effects of 3D structure are strong, 2D inversion will become insufficient. Therefore, we must also discuss the possibility of extending the method to 3D inverse problems. The rapid progress in computers has recently made it possible to solve the 3D problems. However, this does not imply that the 3D inverse problems, especially the nonlinear inverse problems, can be solved immediately for the following reasons. First, in order to perform an inversion, the forward problems have to be solved repeatedly, which takes a long time. Second, the parameters to be estimated in a 3D inverse problem are increased by square compared with those in a 2D inverse problem. Moreover, we face a difficulty in obtaining data from many surface stations to cover a target area. The method proposed in this study will have certain advantages over other conventional methods when it becomes possible to solve 3D forward problems within a reasonable computation time and to challenge the 3D inverse problems. First of all, the use of the full waveform enables us to perform the inversion with data from less stations, when compared with the methods that employ only the direct waves. Moreover, compared with a conventional method such as the tomography, in which the parameters have to be estimated at all grid points, the number of parameters to be estimated is much less in our method. By extending equation (4), the representation of the boundary shape in a 2D problem and a 3D problem is represented as

$$\zeta(x, y) = \zeta^0(x, y) + \sum_{i,j} p_{ij} \times c_{ij}(x, y), \qquad (8)$$

where p_{ij} is a parameter that represents the boundary shape and

$$c_{ij}(x, y) = c_i(x)c_j(y). \qquad (9)$$

The right side of this equation is a basis function defined in equation (3).

One difficulty of extending our inversion method to the 3D problem, and also to the 2D *P-SV* problem, is the evaluation of the incident wave field. While a simple *SH* plane wave is assumed in this study, the incident wave field in reality consists of *P* waves, *S* waves, and surface waves, which makes it necessary to separate them. One possible solution to evade this problem would be the introduction of a point source. In any case, the high possibility of extending our inversion method to the 2D *P-SV* problems and the 3D problems has to be emphasized.

Conclusions

We developed a method for estimating the boundary shape of a basin structure using waveform inversion. We formulated a boundary shape waveform inversion for the case of a plane *SH* wave impinging on a two-layered structure and examined the validity of that inversion with numerical experiments.

The boundary shape of the entire basin could be estimated almost perfectly from records taken from only a small number of surface stations by using the full waveform, including the later phases, when an appropriate initial model is given. When the value of $\Delta\zeta_{max}$ is large, which means that the initial model is inappropriate, the computation becomes unstable. In such cases, stable computation may be obtained by a hierarchical scheme of inversion that consists of gradually increasing the number of model parameters. To check the effects of errors on the inversion, we investigated cases of data containing noise and cases of given parameters containing errors. Although errors do affect the inversion, the structure can be estimated roughly as long as the errors are not very large (noise in the records less than 15% and the errors of *S*-wave velocity and the incident angle respectively within 5% and 5°).

Our simple assumption of a two-dimensional, two-layered structure and an *SH* wave field does not stem from any essential difficulty. The method described, therefore, can be expanded to more general problems, such as the *P-SV* wave field.

Acknowledgments

We thank Hiroshi Kawase, Hiroshi Takenaka, and Hiroyuki Fujiwara for their most helpful suggestions. We are also grateful for the discussion and useful advice provided by Yoshimasa Kobayashi, Shoichi Kobayashi, Masanori Horike, and Yuzo Shinozaki. We acknowledge the critical reviewing of Charles Ammon, John Cassidy, and an anonymous referee.

References

Aki, K. and K. L. Larner (1970). Surface motion of a layered medium having an irregular interface due to incident plane SH waves, *J. Geophys. Res.* **75**, 933–954.

Aki, K. and P. G. Richards (1980). *Quantitative Seismology: Theory and Methods*, W. H. Freeman and Co., San Francisco, California.

Ammon, C. J., G. E. Randall, and G. Zandt (1990). On the nonuniqueness of receiver function inversions, *J. Geophys. Res.* **95**, 15303–15318.

Bard, P. Y. and M. Bouchon (1980). The seismic response of sediment-filled valleys. Part 1: the case of incident SH waves, *Bull. Seism. Soc. Am.* **70**, 1263–1286.

Barone, M. R. and D. A. Caulk (1982). Optimal arrangement of holes in a two-dimensional heat conductor by a special boundary integral method, *Int. J. Numer. Meth. Eng.* **18**, 675–685.

Beck, J. L. and J. F. Hall (1986). Factors contributing to the catastrophe in Mexico City during the earthquake of September 19, 1985, *Geophys. Res. Lett.* **13**, 593–596.

Boore, D. M. (1972). Finite difference methods for seismic wave propagation in heterogeneous materials, in *Methods in Computational Physics*, B. A. Bolt (Editor), Vol. 11, Academic Press, New York.

Haskell, N. A. (1953). The dispersion of surface waves in multilayered media, *Bull. Seism. Soc. Am.* **43**, 17–34.

Horike, M. (1987). Extension of the Aki and Larner method to absorbing media with plural curved interfaces and several characteristics of a seismic response on a sedimentary basin, Zisin second series, *J. Seism. Soc. Japan* **40**, 247–259 (in Japanese with English abstract).

Kawase, H. and K. Aki (1989). A study on the response of a soft basin for incident S, P, and Rayleigh waves with special reference to the long duration observed in Mexico City, *Bull. Seism. Soc. Am.* **79**, 1361–1382.

Kubo, S. (1992). *Inverse Problems*, Baifukan, Tokyo (in Japanese).

Kubo, S., T. Sakagami, K. Ohji, T. Hashimoto, and Y. Matsumuro (1988). Quantitative measurement of three-dimensional surface cracks by the electric potential CT method, *J. Mech. Soc. Japan* A-**54**-498, 218–225 (in Japanese with English abstract).

Nakagawa, T. and Y. Oyanagi (1982). *Experimental Data Analysis by the Least-Squares Method*, Univ. of Tokyo Press, Tokyo (in Japanese).

Nishimura, N. and S. Kobayashi (1991). A boundary integral equation method for an inverse problem related to crack detection, *Int. J. Numer. Meth. Eng.* **32**, 1371–1387.

Nowack, R. L. and L. W. Braile (1993). Refraction and wide-angle reflection tomography: theory and results, *Seism. Tomography: Theory and Practice*, 733–763.

Olsen, K. B. (1989). A stable and flexible procedure for the inverse modelling of seismic first arrivals, *Geophys. Prospecting* **37**, 455–465.

Ricker, N. H. (1977). Transient waves in visco-elastic media, Amsterdam.

Sánchez-Sesma, F. J. and J. A. Esquivel (1979). Ground motion on alluvial valleys under incident plane SH waves, *Bull. Seism. Soc. Am.* **69**, 1107–1120.

Sánchez-Sesma, F. J., J. Ramose-Martínez, and M. Campillo (1993). An indirect boundary element method applied to simulate the seismic response of alluvial valleys for incident P, S and Rayleigh waves, *Earthquake Eng. Struct. Dyn.* **22**, 279–295.

Smith, W. D. (1975). The application of finite element analysis to body wave propagation problems, *Geophys. J. R. Astr. Soc.* **42**, 747–768.

Tanaka, M. and K. Yamagiwa (1988). Application of boundary element method to some inverse problems in elastodynamics, *J. Mech. Soc. Japan* A-**54**-501, 1054–1060 (in Japanese with English abstract).

White, D. J. (1989). Two-dimensional seismic refraction tomography, *Geophys. J.* **97**, 223–245.

Yamanaka, H., K. Seo, and T. Samano (1989). Effects of sedimentary layers on surface-wave propagation, *Bull. Seism. Soc. Am.* **79**, 631–644.

Yamanaka, H., K. Seo, and T. Samano (1992). Analysis and numerical modeling of surface-wave propagation in a sedimentary basin, *J. Phys. Earth* **40**, 57–71.

Disaster Prevention Research Institute
Kyoto University
Gokasho, Uji
Kyoto 611, Japan
(S.A., T.I., K.I.)

Instituto de Ingenieria
UNAM Cd. Universitaria Apdo.
70-472 Coyoacan 04510 México, D.F. México
(F.J.S.-S.)

Manuscript received 20 August 1993.